Control strategies for the suppression of flame instabilities

van den Boom, J.D.B.J.

Award date:
2004

Control strategies for the suppression of flame instabilities

J.D.B.J. van den Boom

DCT 2003.97

Master's thesis

Coach: Dr. K.R.A.M. Schreel

Supervisor: Prof. Dr. H. Nijmeijer, Prof. Dr. L.P.H. de Goey

Graduation Committee: Prof. Dr. H. Nijmeijer, Prof. Dr. L.P.H. de Goey, Dr. K.R.A.M. Schreel and Dr. Ir. I. Lopez

Technische Universiteit Eindhoven
Department Mechanical Engineering
Dynamics and Control Technology Group

Eindhoven, November, 2003

Abstract

Combustion of premixed flames is applied in for instance central-heating boilers. One of the problems of this application is that premixed flames are unstable by nature. Flat flames stabilised on a burner (applied in central-heating boilers) can sometimes oscillate spontaneously. Self-sustained oscillations result from a coupling between unsteady combustion and acoustic waves within the combustor, described by the Rayleigh criterion. Besides if these flames are placed in an external acoustic field they will show resonating fluctuations, as a result of which the flame will act as a sound amplifier. These phenomena are not desirable, because under some circumstances the central-heating boiler will produce an inadmissible quantity of sound.

The possibility of (active) suppression of these oscillations through feedback control is investigated in this thesis. First of all a differential equation with time delay is derived based on the G-equation. The G-equation is a kinematic equation, describing the (rigid) motion of a flame. The differential equation describes the relation between the fluctuations in total heat-release and external (acoustic) disturbances.

Then the used closed-loop control strategy, linear $\mathcal{H}_\infty$ control, is introduced. The choice for this model-based strategy originates from the performance challenges (disturbance attenuation and the high degree of uncertainties in combustion systems). A controller is synthesised after a Padé approximation is done for the time delay. This results in a rational model. When the stability of the system is investigated, it is seen that as a result of the approximation poles turned up in the right-half plane. This means that the system is unstable. The $\mathcal{H}_\infty$ controller is not able to stabilise the system. Therefore, the poles are placed with a proportional controller in the left-half plane. For this new system, consisting of the rational model and the proportional controller, a $\mathcal{H}_\infty$ controller is designed. This controller has to make sure that there is disturbance attenuation. This is evaluated during simulations.

Finally the performance of the controller is evaluated during experiments. To be able to judge the performance, first a phase-delay controller is tested. This control strategy leads to a reduction of the fluctuations in heat release. From thorough testing of the $\mathcal{H}_\infty$ controller can be concluded that this strategy has not worked yet. A possible explanation can be found in the fact that the fluctuations in heat-release are too big, thus linearisation was not allowed.

Samenvatting

Verbranding in voorgemengde vlammen wordt onder andere toegepast in CV-ketels. Een nadeel van voorgemengde vlammen bij deze toepassing is dat ze van nature instabiel zijn. Een vlakke (voorgemengde) vlam kan gestabiliseerd op een vlakke poreuze brander spontaan oscilleren. Spontane oscillaties zijn het gevolg van een relatie tussen instabiele verbranding en geluidsgolven in de CV-ketel. Deze relatie wordt ook wel het Rayleigh criterium genoemd. Bovendien kan de vlam als geluidsversterker optreden in een extern akoestisch veld. De vlam vertoont dan 'resonante' oscillerende bewegingen. Beide verschijnselen zijn niet gewenst, omdat het apparaat dan een ontoelaatbare hoeveelheid geluid kan produceren.

In deze studie wordt onderzocht of het mogelijk is om deze oscillaties actief te onderdrukken met behulp van feedback regelaars. Allereerst is er een differentiaalvergelijking met tijdsvertraging afgeleid op basis van de G-vergelijking. De G-vergelijking geeft een kinematische beschrijving voor een 'star' bewegende vlam. De differentiaalvergelijking beschrijft de relatie tussen fluctuaties in afgifte van warmte door de vlam en externe (akoestische) verstoringen.

Hierna is de gebruikte feedback regelstrategie, $\mathcal{H}_\infty$ control, besproken. De vereiste prestaties (onderdrukking van verstoringen en onzekerheid in modellering) van de regelaar hebben geleid tot de keuze van deze model-gebaseerde strategie. Een regelaar is bepaald nadat het model rationeel gemaakt is, door de tijdsvertraging met een Padé benadering te beschrijving. Echter als gekeken wordt naar de stabiliteit van het systeem dan heeft de benadering er voor gezorgd dat er polen in het rechter halfvlak terecht gekomen zijn, en er dus sprake is van een instabiel systeem. De $\mathcal{H}_\infty$ regelaar is niet in staat om het systeem te stabiliseren. Daarom zijn eerst de polen met behulp van en proportionele regelaar verplaatst naar het linker halfvlak. Voor dit nieuwe systeem, bestaande uit het rationele model en de proportionele regelaar, is een $\mathcal{H}_\infty$ regelaar, die moet zorgen voor de verstoringsonderdrukking, afgeleid. De werking van deze regelaar is beoordeeld tijdens simulaties.

Vervolgens is de prestatie van de regelaar beoordeeld tijdens experimenten. Om de prestaties te kunnen beoordelen is allereerst een fase-vertragende regelaar getest. De regelactie leidt tot een halvering van de fluctuaties van de afgifte van warmte door de vlam. Uit uitvoering testen van de $\mathcal{H}_\infty$ regelaar kan geconcludeerd worden dat deze nog niet werkt. Een mogelijke oorzaak kan zijn de fluctuaties in warmte-afgifte te groot zijn en dat er geen linearisatie had plaats mogen vinden.

Contents

Nomenclature

Roman Characters

symbol	description	units
A	states matrix	-
B	input matrix	-
C	output matrix	-
c_p	specific heat (capacity) at constant pressure	J/(kgK)
D	direct transmission matrix	-
E_a	activation energy	J/mole
f	frequency	1/s
$G(s)$	transfer function	-
H	total specific enthalpy	J/kg
ΔH	combustion enthalpy	J/kg
J	specific enthalpy	J/kg
m	mass burning rate	kg/(m^{2}s)
p	pressure	Pa
Q_rel	heat release	J/(m^{2}s)
R	gas constant	J/(kg K)
T_a	activation temperature	K
T_ad	adiabatic flame temperature	K
T_b	flame temperature	K
T_u	ambient temperature	K
s	Laplace variable	-
t	time	s
u	velocity	m/s
u	control command	-
v	measurement	-
w	exogenous inputs	-
x	spatial coordinate	m
x_f	stand-off distance	m
Y_i	mass fraction	-
Z	flame 'feed-back' coefficient	-
z	exogenous outputs	-
ω	(angular) frequency	rad/s
OH*	amount of radiated OH	-
Le	Lewis number	-
Ma	Mach number	-
Ze	Zeldovich number	-

Greek characters

symbol	description	units
δ	flame thickness	m
λ	heat conductivity	J/(m s K)
ρ	density	kg/m^3
ρ_i	partial density	kg/m^3
$\dot{\rho}_i$	reaction rate	kg/m^3
$\overline{\sigma}$	maximal singular value	-
τ	time delay	s
τ_f	flame time	s
ϕ	mass flow rate	$kg/(m^2s)$
ψ	density weighted spatial coordinate	m
ψ_f	density weighted stand-off coordinate	m
ω	(angular) frequency	rad/s

Subscript

$()_b$ burned
$()_g$ gas
$()_s$ solid
$()_u$ unburned

Superscript

$\overline{()}$ steady part of a quantity
$()'$ time dependent part of a quantity

Acknowledgement

The work presented in this thesis was conducted in the Department of Mechanical Engineering between September 2002 and October 2003. During this time frame, I received support from many sources.

To thank people should be done properly, for every person on a suitable way. Therefore thanking people via this section of my report, will not suffice, at least not for me. However it is written proof. I will nevertheless name all people to which I am thankful.

First of all I am greatly indebted to my coach, Dr. Koen Schreel and to my supervisors Prof. Dr. Henk Nijmeijer and Prof. Dr. Philip de Goey, for their guidance and encouragement throughout the course of my Master Thesis.

Secondly I express my sincere thanks to Ing. Edwin van de Tillaart, who provided technical help during the experimental (and numerical) phase of the present work.

Last but not least I am very grateful to my friends and my family, particularly, my parents, my brother and my sister for their encouragement and love.

Joris van den Boom
October 2003

Note that there also is a version of this report at the Division of Thermal Fluid Engineering, Combustion Technology Section. This report has the report number *WVT 2003.10.*

Chapter 1

Introduction

1.1 Motivation for active control

The occurrence of combustion instability has long been a subject of interest in continuous combustion systems. Continuous combustion processes are encountered in applications related to power generation, propulsion and heating. The term combustion instability refers to a wide variety of oscillatory phenomena observed in combustion systems. Unstable combustion is unwanted and is associated with (high) pressure fluctuation levels (observes as humming and whistling noises in modern central-heating boilers) and enhanced heat release to the combustor boundaries. Such conditions are detrimental to the performance of the combustor, and in worst case, can cause structural damage.

In order to meet the very strict emission requirements, modern central-heating boilers have been equipped with fully premixed surface burners. Completely premixed flames stabilised on a poreus or perforated burner deck are effectively cooled, which lead to low nitrogen oxide (NO_x) emission. The formation of NO_x happens at high temperatures. A disadvantage of this type of boiler is the sensitivity to acoustic instabilities. The noise problem has become complex due to the varying burner loads, which influence the acoustic properties of the system.

Essentially, self-excited combustion oscillations result from a coupling between unsteady combustion and acoustic waves within the combustor. The unsteady rate of the heat release is very sensitive to oncoming flow disturbances. Since unsteady combustion is an efficient acoustic source [Dow83], a self-excited oscillation is possible, where the unsteady combustion generates acoustic waves which are reflected at the combustor boundaries and come back to perturb the flame further (monopole source). If the phase relationship between unsteady heat release and pressure is suitable, acoustic energy will be produced. (The so-called Rayleigh criterion [Roo01]) In practice, many other complex mechanisms can be involved and lead to unstable combustion, such as hydrodynamic instabilities and intrinsic flame instabilities.

In order to mitigate the combustion instabilities and hence extend the stable operating range of combustion systems, passive control techniques, including ad hoc modifications of the fuel injection system and burner geometry and enhancement of passive acoustic damping have been investigated and are currently been used. However passive control is often inadequate under fluctuating operating conditions.

Active control is an alternative manner of interrupting the damaging interaction between acoustic waves and unsteady combustion. 'Active' means that continuously a (specific) combustion parameter is perturbed via an actuator. The actuator can either affect the acoustic field or modify directly the unsteady heat release rate. In acoustic modulation, a driver, in general a loudspeaker, is used to modulate the pressure field and as a result of this alter the flow rate and/or the fuel-air mixing pattern before entering the flame front. Modulation of fuel supply alters the fuel flow stream directly into the burner, in a manner that the heat released by the flame is not coupled anymore with the acoustic characteristics of the chamber.

Active control can be in an open-loop or in a closed-loop configuration. In the former, the control action does not depend on the combustor's response to the control action. (There is no measurement of the output and no subsequent use of that output to make the system conform to the desired output.) While in the latter, the controller drives the actuator in response to a sensor measurement. A demonstration of the effectiveness of closed-loop, also called feedback control applied to combustion oscillations is reported by for instance Poinsot *et al.* [Poi87] or more recently by Evesque *et al.* [Eve03]. Both used a loudspeaker as an actuator. Examples of the success of modulating the fuel supply can be found in Langhorne *et al.* [Lan90] or Campos *et al.* [Cam03].

To be employable in practice, an active controller needs to be effective at different operating conditions, i.e. the controller has to be robust with respect to the heat released by the flame and the ratio of fuel to oxidiser in the premixed flame. An efficient approach might be to use a $\mathcal{H}_\infty$ controller, which can only be efficient in the frame of feedback control.

1.2 Control challenges

The control of combustion instabilities has still a number of challenges. These challenges can be classified in two categories: control concept challenges and performance challenges.

1.2.1 Control concept challenges

1. The driving mechanism of the instability, the complex interactions between acoustics and combustion. There are several ways to model the interaction between acoustics and combustion, for instance the models derived by Fleifil *et .al* [Fle96] and Dowling [Dow99]. These are physically-based low-order models based on flame surface kinematics. The kinematics are modelled using the G-equation. On the other hand, there are models derived through frequency domain identification (measurements), like the model of Campos *et al.* [Cam03]. In this thesis the model will be designed using the G-equation as will be shown in Chapter 2. This model should be a reliable presentation of the reality, because the controller will be synthesised using a model-based technique.

2. Safety-critical control design will play a role in the application of active control of combustors. It is highly desirable that the controller provides some guarantee that the system will not become unstable and cause harm.

1.2.2 Performance challenges

1. The combustion system to be controlled will suffer from substantial time delays, due to acoustic wave propagation, enthalpy waves growth, etc. This will be explained in chapter 2. These delays affect the control action and should be taken into account in the control design;

2. The flow in the combustor, in the current study, is laminar, so robustness to background noise is not a big issue compared to turbulent flows, but noise must be controlled;

3. At unstable operating conditions, oscillations can grow rapidly, i.e. in a few milliseconds. The controller response needs to be (very) fast;

4. The control effort should be as small as necessary to achieve the required performances on the combustion system. A limitation on the control effort allowed needs to be investigated and included in the control design.

5. For practical implementations, control algorithms should be as simple as possible and require only real-time measurement;

1.3 Objectives and summary of research programme

The objective of this thesis is to investigate if it is possible to suppress the combustion oscillations of flames stabilised on flat surface burners actively through feedback control. In particular,

- In a first step, it is necessary to provide some insight into the combustion instability phenomenon. The Rayleigh criterion plays an important role in the understanding of combustion instabilities and will therefore be introduced. Further a model for the flame motion will be derived. This is the subject of chapter 2;
- The control problem will be formulated and the used strategy will be explained. For computational reasons a state-space notation for the flame dynamics will be derived and in order to cope with time delay a Padé-approximation for the time delay will be used. Finally a controller will be derived and evaluated using simulations. This is the subject of chapter 3;
- In chapter 4 the test-rig and the measurement principles will be discussed. After system identification a new controller can be derived and evaluated during experiments.
- The report will be concluded in chapter 5. The achievements of the present research are summarised and recommendations for future research are made.

Chapter 2

Flame dynamics

2.1 The Rayleigh Criterion

Self-excited oscillations in a central-heating boiler belong to the field of thermoacoustics which deals with the interaction between heat and sound. Pressure waves can be produced by a fluctuating heat-release in an acoustic medium like a gas-mixture. These pressure waves alter on their turn the heat-release, closing the loop, see Figure 2.1. The heat-driven acoustic oscillations can be divided into convection/conduction-driven oscillations and combustion-driven oscillations [Roo01].

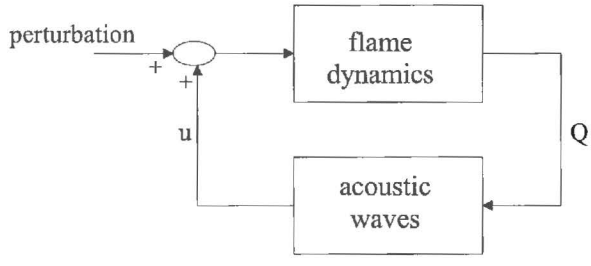

Figure 2.1: *Feedback scheme for self-excited oscillations*

At the end of the eighteenth century, combustion-driven oscillations were recognised by Higgins. Sound was produced while setting a flame inside an open or closed-ended tube. This phenomenon was called the singing flame. The Rijke tube, an example of a convection/conduction-driven oscillation, was invented in 1859 by placing a hot gauze in the lower half of an open-ended vertical tube. It was observed that the sounded oscillations were stronger or weaker while placing the heat-source at different locations in the tube. Lord Rayleigh explained the development of heat-driven oscillations. He first explained how the addition of heat affects sound waves. If heat is added to a sound wave when it is at the high temperature phase of its cycle, energy is fed into the acoustic disturbance. When heat is added at the low temperature limit the sound wave loses energy. Since the compression in a sound wave is adiabatic the pressure and temperature fluctuations have to be in phase. Heat addition during a positive pressure disturbance increases the amplitude of the sound waves, but it has the opposite effect when the pressure disturbance is negative [Dow83]. This is later translated in the Rayleigh Criterion.

$$\int_0^\tau \int_0^V p'(\vec{x},t)q'(\vec{x},t)d\vec{x}\,dt > 0, \tag{2.1}$$

where p' and q' are the perturbations in pressure and heat-release, respectively. The period of oscillation is τ and V is the combustor volume. The left-hand side of inequality (2.1) indicates that to satisfy the Rayleigh Criterion a specific relationship between p' and q' must exist. Assuming

that p' and q' have a periodic time dependence, the sign of the time integral of their product will depend on the ratio τ_0/τ, with τ_0 the phase difference between the perturbation in pressure and heat-release. A straightforward evaluation of the (time) integral shows that it has a maximum (positive), when $\tau_0/\tau = 0, 1, 2..$ and a minimum (negative), when $\tau_0/\tau = \frac{1}{2}, \frac{3}{2}...$ This is conform to the Rayleigh hypothesis: p' and q' in phase will lead to instability. On the other hand, when p' and q' are out of phase, the effect will be a stabilising one. Note that the integrals are also spatial, which means that destabilising and stabilising can occur in different locations of the combustor. In this thesis only temporal fluctuations in pressure and heat- release are considered, as often done in literature, because the length scale of the premixed flat flame is much smaller than the acoustic length scale. The speed at which sound waves travel through small areas, as can be found in central-heating boilers, can be considered infinitely high. Therefore, on the flame scale the acoustic wave is independent of the spatial coordinate.

2.2 Equation of Motion

Before a model can be derived that describes the behavior of a flat burner-stabilised premixed flame in an acoustic field a number of assumptions have to be made:

- Premixed means that the fuel (methane) and oxidiser (air) are mixed before combustion. The (fuel) equivalence ratio, Φ, is characteristic for the amount of fuel and oxidiser, and is defined as:
$$\Phi = \frac{2X_{\mathrm{CH_4}}}{X_{\mathrm{O_2}}}, \tag{2.2}$$
where $X_{\mathrm{CH_4}}$, $X_{\mathrm{O_2}}$ are the mole fractions in the unburnt mixture. Only mixtures with $\Phi < 1$, i.e. lean mixtures, are considered;

- Acoustic energy can only be transported by plane waves, because of that it is sufficient to consider one-dimensional disturbances. This is supported by the fact that in a ducted system, like a central-heating boiler, the cross-flow dimensions are much smaller than the wave lengths present in the acoustic field. (The frequencies of interest are low (< 1000Hz).) Further is assumed that the flow at the inlet is isentropic;

- The Mach number of the flow is low ($O(10^{-4})$), which means that across the flame pressure variations are negligible. This justifies the use of the set of low-Mach number equations. The Mach number (Ma) is defined as the ratio u/c, with u the flow velocity and c the speed of sound. Thus $p'_{\mathrm{u}} = p'_{\mathrm{b}}$, where the subscript $_{\mathrm{u}}$ denotes the unburned (upstream) side of the flame, the subscript $_{\mathrm{b}}$ denotes the burned (downstream) side of the flame;

- The diffusivity of fuel is equal to the diffusivity of heat, that is the Lewis number is 1 and all species have constant and equal specific heats ($c_{\mathrm{p}} = \bar{c}_{\mathrm{p}}$).

In general the starting point of the description of gaseous combustion processes will be the conservation of mass, species mass fractions, energy and momentum. However in this thesis the beginning is a quasi-stationary equation, describing a relation between the flame temperature, T_{b}, and the mass burning rate, $m_{\mathrm{u}}(x,t)$.

2.2.1 Acoustics and stability without damping

A variation in flame temperature is assumed to result in an instantaneous change in the mass burning rate $m = \rho_{\mathrm{u}} s_{\mathrm{L}}$. The burning velocity is s_{L}, ρ_{u} is the density. It is assumed that the flame behaves as a rigid oscillating structure, which implies that the mass burning rate is a function of time only. The spatial dependence of the density is eliminated by introducing density-weighted coordinates or von-Mises coordinates:

$$\psi(x,t) = \frac{1}{\bar{\rho}_u}\int_0^x \rho(\xi,t)\mathrm{d}\xi \quad \text{and} \quad \tau(x,t) = t,$$

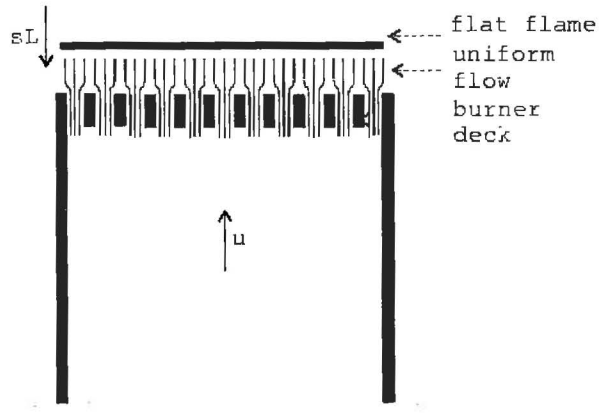

Figure 2.2: *schematic cross section of a burner with stabilised flame, Figure adopted with permission from the master thesis of R.W.M. Janssen*[Jan02]

where the bar denotes the steady part of a quantity and τ is the time coordinate. The von-Mises space variable is ψ. The relation between T_b and m is then given by:

$$\frac{\partial m(\tau)}{\partial \tau} = \frac{\mathrm{Ze}}{2} \frac{\overline{m}}{(\overline{T}_\mathrm{b} - T_\mathrm{u})} \frac{\partial T_\mathrm{b}}{\partial \tau}, \tag{2.3}$$

where Ze is the Zeldovich number, T_u is the temperature of the burner. This relation is adopted from the Goey [Goe03]. The Zeldovich number is a measure for the sensitivity of the burning velocity s_L to perturbations of the maximal temperature, described by:

$$\mathrm{Ze} = E_\mathrm{a} \frac{T_\mathrm{b} - T_\mathrm{u}}{R T_\mathrm{b}^2},$$

with the activation energy E_a, and the universal gas constant R. The Zeldovich number is the only information of the chemical reaction mechanism that is required in this model. As the mass fraction of fuel $Y = 0$ at the flame front $\psi = \psi_\mathrm{f}$, equation (2.3) can also be written as:

$$\frac{\partial m(\tau)}{\partial \tau} = \frac{\mathrm{Ze}}{2} \frac{\overline{m}}{(\overline{T}_\mathrm{b} - T_\mathrm{u})} \frac{\partial J(\psi_\mathrm{f}, \tau)}{\partial \tau},$$

where dJ, a change in the 'total enthalpy' in the system is given by:

$$dJ = \Delta H dY + c_p dT,$$

with ΔH the combustion enthalpy, Y the mass fraction of the fuel. Fluctuations in enthalpy (J) will be transported with a wave with a wave velocity equal to the gas velocity u_u. Therefore, heat losses to the burner at $\psi = 0$ are noticed at the flame front $\psi = \psi_\mathrm{f}$ with a time lag. This means that the enthalpy does not only depend on time, but also on space coordinate ψ. Furthermore, due to damping effects, the shape of the enthalpy waves will change while it travels. To formulate a general solution for this wave dispersion behavior is difficult. Therefore damping will first be neglected (the shape of the enthalpy fluctuations will stay the same). $\partial J(\psi_\mathrm{f}, \tau)/\partial \tau$ can be replaced by:

$$\frac{\partial J(\psi_\mathrm{f}, \tau)}{\partial \tau} = \frac{\partial J(0, \tau - \psi_\mathrm{f}/u_\mathrm{u})}{\partial \tau} = \Delta H \frac{\partial Y(0, \tau - \psi_\mathrm{f}/u_\mathrm{u})}{\partial \tau}. \tag{2.4}$$

In the last step it is assumed that at $\psi = 0$, T is constant and equal to the burner temperature.

2.2.2 The G-equation

If the flame is stationary the gas velocity $\overline{u}_u$ equals the (laminar) burning velocity $\overline{s}_L$ or $\overline{m} = \rho_u \overline{s}_L = \rho_u \overline{u}_u = \overline{\phi}_u$, with $\overline{\phi}_u$ the stationary mass flow rate. (This is only valid for one-dimensional flames.) In case of an unstable flame, there will be no equilibrium between u_u and s_L. Therefore the velocity of the flame front, $u_f = u_u - s_L$, is unequal to zero. A possibility to describe the equation of motion of the premixed flame is by using the G-equation:

$$\frac{\partial G}{\partial t} + \vec{u} \cdot \nabla G = s_L |\nabla G|$$

This equation is derived from a purely kinematic relation:

$$\frac{dx_f}{dt} = u(x_f, t) + s_L n(x, t)$$

between the displacement of the flame front (x_f), local velocity and burning velocity normal to the flame front. A scalar field G can be defined, so that $G = G_0$ on the flame front, $G < G_0$ in the unburned region and $G > G_0$ in the burned region. The iso-contours with a constant G can be seen as a lines with equal height. If the flame moves the G-field will also move, thus $G = G_0$ will stay constant on the flame front. (Figure 2.3)

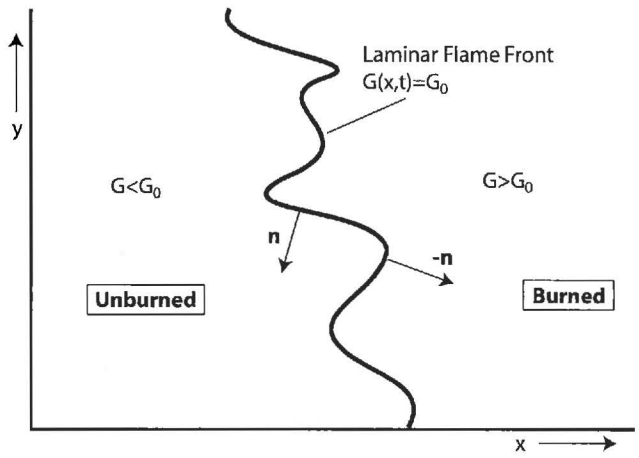

Figure 2.3: *G-field for the definition of the flame front*

The G-equation, will be solved for the flame motion in terms of methane mass fraction Y.

$$\rho_u \frac{\partial Y}{\partial \tau} + \phi_u(\tau) \frac{\partial Y}{\partial \psi} = m_u(\tau) \frac{\partial Y}{\partial \psi} \tag{2.5}$$

Due to heat loss at the burner, it is not allowed to follow a similar procedure for the temperature. Since the temperature is constant ($T = T_u$) at the burner, variations in the enthalpy appear at the burner outlet. These enthalpy variations are transported to the reaction zone by convection and diffusion, where they lead to flame temperature variations. In turn, these variations induce variations in the mass burning rate m, which influence the flame motion through the G-equation. This feedback mechanism can cause resonant flame motion.

Substituting (2.4) and (2.5) in (2.3) yields:

$$\frac{\partial m(\tau)}{\partial \tau} = \frac{Ze}{2} \frac{\overline{u}_u}{c_p(\overline{T}_b - T_u)} \Delta H \frac{\partial Y(0, \tau - \psi_f/u_u)}{\partial \psi} (m(\tau - \psi_f/u_u) - \phi_u(\tau - \psi_f/u_u)) \tag{2.6}$$

Small acoustic perturbations in $\frac{\partial Y}{\partial \psi}(0, \tau - \psi_f/u_u)$ are neglected since they will be of higher-order in the acoustic distortion. It is possible to express the gradient $\partial Y(0)/\partial \psi$ in terms of stationary

flame heat loses:

$$\Delta H \frac{\partial Y}{\partial \psi}(0, \tau - \psi_f/u_u) = -\frac{c_p(T_{ad} - \overline{T}_b)}{\delta},$$

where $\delta = \overline{\lambda}_u/(\overline{\phi}_u c_p)$ is the flame thickness. This gives for equation (2.6):

$$\frac{\partial m(\tau)}{\partial \tau} = (\phi_u(\tau') - m(\tau'))\frac{Ze}{2}\frac{\overline{u}_u}{\delta}\left(\frac{T_{ad} - \overline{T}_b}{\overline{T}_b - T_u}\right),$$

with $\tau' = \tau - \psi_f/$
$overline{u}_u$, the delayed time. The previous equation can be written as a first order differential equation:

$$\frac{\partial m_u(\tau)}{\partial \tau} + \frac{Z}{\tau_f} m_u(\tau') = \frac{Z}{\tau_f}\phi_u(\tau'), \tag{2.7}$$

where the 'flame time' is defined by $\tau_f = \delta/\overline{u}_u$ and the flame 'feed-back' coefficient given by:

$$Z = \frac{Ze}{2}\left(\frac{T_{ad} - \overline{T}_b}{\overline{T}_b - T_u}\right)$$

A relation between the fluctuating (total) heat-release, Q'_{rel}, and the fluctuating mass burning rate is given by:

$$Q'_{rel}(\tau) = c_p(\overline{T}_b - \overline{T}_u)m'(\tau) \tag{2.8}$$

Substituting equation (2.8) in equation (2.7) and using $\phi'_u(\tau) = \rho_u u'_u(\tau)$ yields:

$$\frac{\partial Q'_{rel}(\tau)}{\partial \tau} + \frac{Z}{\tau_f} Q'_{rel}(\tau') = \frac{Z}{\tau_f}\frac{\rho_u}{c_p(\overline{T}_b - \overline{T}_u)} u'_u(\tau') \tag{2.9}$$

The Laplace transform, a transformation from the time domain into the complex frequency domain, is defined as:

$$X(s) = \int_0^\infty x(t)\exp(-st)dt,$$

where s is the Laplace variable. ($s \in \mathbb{C}$) After taking the Laplace transform of equation (2.9) it is possible to derive a relation (transfer function) between the fluctuations in gas velocity $U(s)$, the right hand side of equation (2.9) and the fluctuations in heat-release $Q(s)$. The Laplace transformation is given by:

$$\frac{Q(s)}{U(s)} = \frac{\rho_u c_p(\overline{T}_b - \overline{T}_u)}{\frac{\tau_f}{Z} s\exp(s\frac{\psi_f}{\overline{u}_u}) + 1}, \tag{2.10}$$

Figure 2.4 shows the Frequency Response Function (FRF) plot (behavior of amplitude and phase) of the equation of motion (2.10). The following values have been used for Figure 2.4: an equivalence ratio of $\Phi = 0.8$, and the gas velocity $\overline{u}_u = 14$ cm/s. The mixture has a density of $\overline{\rho}_u = 1.131$ kg/m^3, a specific heat of $c_p = 1060$ J/kgK the temperature of the burner is fixed at $\overline{T}_u = 300$ K, the steady flame temperature is $\overline{T}_b = 1836$ K and the adiabatic flame temperature is $T_{ad} = 2013$ K. With an activation energy of 137.173 kJ/mole (one-step chemistry mechanism) the Zeldovich number becomes 13.2.

In Figure 2.5 the FRF plots of the equation of motion (2.10) and the model derived by R. Rook during his Ph.D.-study [Roo01] are shown. In the amplitude graph the same peak can be noticed, only the peak is not so sharp. The phase does not agree. Therefore the phase of equation (2.10) is investigated. (s is replaced by $i\omega$.)

$$\angle\left(\frac{Q(s)}{U(s)}\right) = \angle(\rho_u c_p(\overline{T}_b - \overline{T}_u)) - \angle\left(\frac{\tau_f}{Z} i\omega\exp(i\omega\frac{\psi_f}{\overline{u}_u})\right) + \angle(1) = -\angle\left(\frac{\tau_f}{Z} i\omega\exp(i\omega\frac{\psi_f}{\overline{u}_u})\right)$$

The positive phase change is caused by the fact that the role of the angle of $\exp(i\omega\frac{\psi_f}{\overline{u}_u})$ becomes larger than the angle of $i\omega$.

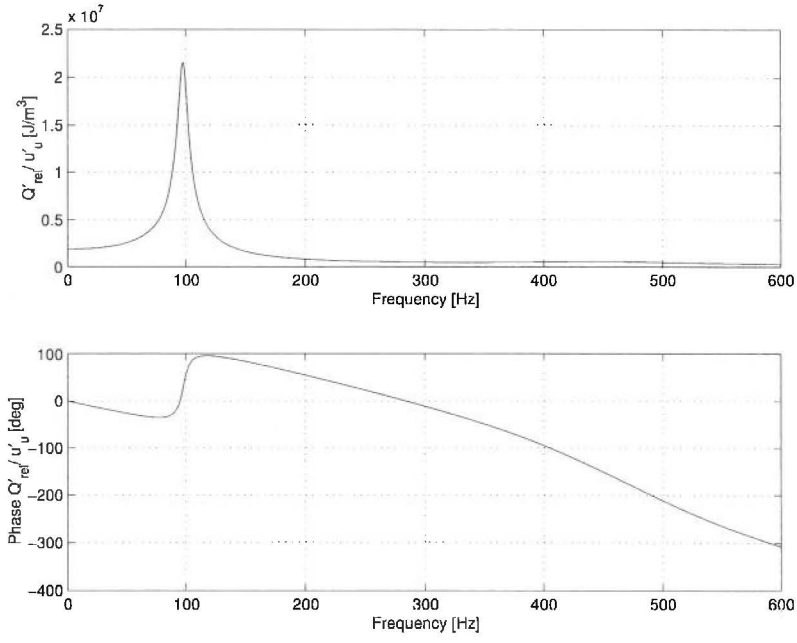

Figure 2.4: *Amplitude and phase of response of total heat-release on the velocity fluctuations*

Note that the definition for ω in flame dynamics differs from the one used in control engineering. In control engineering ω is a real variable, the angular frequency. In flame dynamics ω could be a complex frequency, defined by:

$$\omega = i(\omega_r + \omega_i)$$

The real part of ω (ω_r) is given by $2\pi f$, with f the frequency of oscillation in Hz. *The imaginary part (ω_i) is the damping factor of the oscillation and is considered here to be zero*

2.2.3 Acoustics and stability with damping

Earlier preformed experiments (and numerical observations)[Goe03] have shown that it is not possible with the equation of motion (2.9) to predict stable combustion with a gas velocity lower than 16 cm/s. In a modern central-heating boiler the gas velocity can be lowered to a few cm/s. For this reason it seems appropriate to take the damping of enthalpy waves, as they travel from the burner to the flame, into account. Due to the scattering of enthalpy waves it is not possible anymore to give exact solutions for the model. The analysis is limited to harmonic exponential acoustic distortions (proportional to $exp(i\omega\tau)$) and to exponential solutions of $J(\phi, \tau)$.

For unit Lewis numbers the differential equation for the enthalpy is given by:

$$\rho_u \frac{\partial J}{\partial \tau} + \phi_u \frac{\partial J}{\partial \psi} - \frac{\lambda_u}{c_p} \frac{\partial^2 J}{\partial \psi^2} = 0 \tag{2.11}$$

If damping of enthalpy waves is taken into account equation (2.4) will change to:

$$\frac{\partial J(\psi_f, \tau)}{\partial \tau} = \exp(-\gamma) \frac{\partial J(0, \tau)}{\partial \tau} = \Delta H \exp(-\gamma) \frac{\partial Y(0, \tau)}{\partial \tau},$$

with $\gamma = C\frac{\psi_f}{\delta}$. The parameter C originates from the solution for the fluctuating enthalpy of equation (2.11). For $\partial m(\tau)/\partial(\tau)$ the following expression can be derived:

$$\frac{\partial m(\tau)}{\partial \tau} + \frac{Z \exp(-\gamma)}{\tau_f} m(\tau) = \frac{Z \exp(-\gamma)}{\tau_f} \phi_u(\tau) \tag{2.12}$$

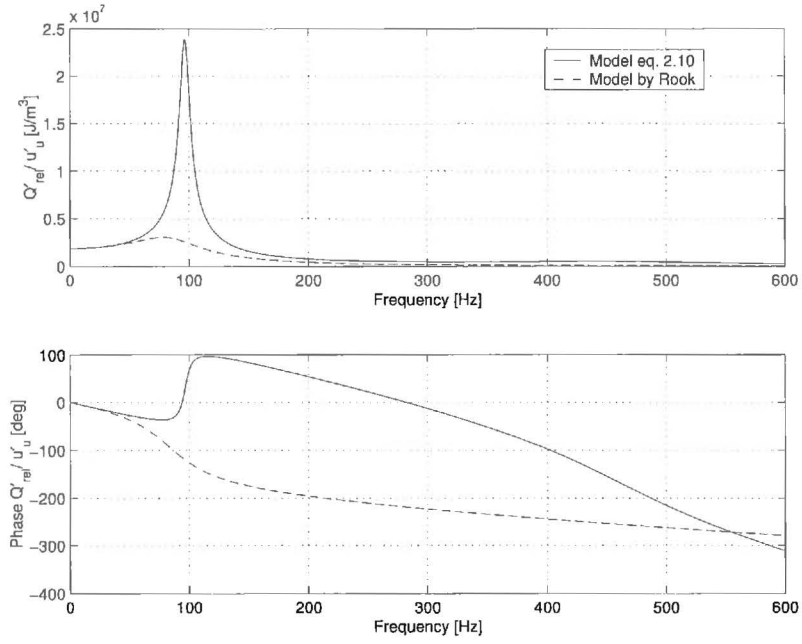

Figure 2.5: *Comparison Model equation (2.10) and Model derived by R. Rook[Roo01]*

After substituting equation (2.8) in equation (2.12), the relation between heat-release and acoustic velocity will be:

$$\frac{\partial Q'_{\mathrm{rel}}(\tau)}{\partial \tau} + \frac{Z}{\tau_{\mathrm{f}}} Q'_{\mathrm{rel}}(\tau) \exp(-\gamma) = \frac{Z}{\tau_{\mathrm{f}}} \rho_{\mathrm{u}} c_{\mathrm{p}} (\overline{T}_{\mathrm{b}} - \overline{T}_{\mathrm{u}}) u'_{\mathrm{u}}(\tau) \exp(-\gamma)$$

Note that the 'delayed' time τ' has been replaced by a phase change $\exp(-\gamma)$.

Equation (2.12 is only valid for exponential solutions, and is for that reason not useable in general. Therefore the damping of enthalpy waves is in the remaining part of this thesis neglected. The model in equation (2.9) will be used to investigate if it is possible to suppress the flame instabilities on flat-surface burners.

2.3 Final Remark

In this chapter a model between the fluctuating heat-release and gas velocity is derived. These parameters are coupled by the mass burning rate. This model describes only the flame dynamics, see Figure 2.1. The relation between gas velocity and heat-release, the acoustic waves, is not modelled, because the controller and actuator will come in place for it. A manner to model the acoustic waves is presented in appendix A.

Chapter 3

The $\mathcal{H}_\infty$ approach to control design

Even before the development of models including combustor dynamics, experimental application of feedback control of combustion instabilities are successfully tested on laboratory-scale systems (mainly loudspeakers are used as actuator). In most cases the 'practical' controller is a proportional feedback or a variation of a PID (proportional-integral-derivate) compensator. One might wonder why that simple approach works or, conversely, ask why a more sophisticated control method is used in this thesis.

The need for a more sophisticated control method, like $\mathcal{H}_\infty$, originates mainly from two aspects: first the performance specifications imposed on the controller, in this case disturbance attenuation. Second, combustion systems show a high degree of uncertainty and variability, and a controller 'tuned' on a particular operating point does not guarantee a reliable performance.

3.1 The background of $\mathcal{H}_\infty$ control

Consider the linear system $G(s)$ in Figure 3.1 with input $u(s)$ and output $y(s)$ (the Laplace transformations of $u(t)$ and $y(t)$ with zero initial conditions):

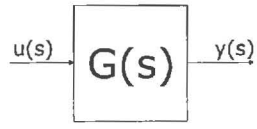

Figure 3.1: *Linear system $G(s)$ with input $u(s)$ and output $y(s)$*

$$y(s) = G(s)u(s)$$

The state-space realisation is an alternative manner of describing the linear system $G(s)$:

$$\dot{x}(t) = Ax(t) + Bu(t), \quad x(t_0) = x_0 \tag{3.1}$$

$$y(t) = Cx(t) + Du(t), \tag{3.2}$$

where $x(t) \in \mathbb{R}^n$ is called the system state, $x(t_0)$ is the initial condition of the system, $u(t) \in \mathbb{R}^m$ is called the system input, and $y(t) \in \mathbb{R}^p$ is the system output. The matrices A,B,C and D are real constant matrices, labelled respectively the system matrix, the input matrix, the output matrix and the direct transmission matrix. Assuming a zero initial state, $x(t_0) = 0$, and taking the Laplace transform of equation (3.1) and (3.2), the transfer function matrix $G(s)$ becomes:

$$G(s) = C(sI - A)^{-1}B + D$$

The system in state-space realisation ((3.1)-(3.2)) has a transfer function representation, but the opposite is not true. For example time delays and improper systems can be represented by Laplace transforms, but they do not have a state-space notation. In improper transfer functions the order of the numerator exceeds that of the denominator.

Observe that the representation in equations (3.1) and (3.2) is not an unique description of the input-output behaviour of the system. First, there exist realisations with the same input-output behaviour but with additional unobservable and/or uncontrollable states. Secondly, even for a minimal representation (a realisation with the fewest numbers of states and consequently no unobservable or uncontrollable states) there are infinite numbers of possibilities.

The dynamical system $\dot{x}(t) = Ax(t) + Bu(t)$, or equivalent the pair (A, B) is said to be state controllable if, for any initial state $x(0)$, any time $t_1 > 0$ and any final state x_1, there exists an input $u(t)$ such that $x(t_1) = x_1$. Otherwise the system is said to be state uncontrollable.

There are several ways to check if a system is state controllable, a possible manner is to look at the controllability matrix:

$$\mathcal{C} \triangleq [\ B \quad AB \quad A^2B \quad \ldots \quad A^{n-1}B\ ]$$

The pair (A, B) is state controllable if and only if the controllability matrix has rank n (full row rank), equal to the number of states.

The dynamical system $\dot{x}(t) = Ax(t) + Bu(t)$, $y(t) = Cx(t) + Du(t)$ (or the pair (A, C)) is said to be state observable if, for any time $t_1 > 0$, the initial state $x(0) = x_0$ can be determined from the time history of the input $u(t)$ and the output $y(t)$ in the interval $[0, t_1]$. Otherwise the system, or (A, C), is said to be state unobservable.

The system (A, C) is state observable if and only if the observability matrix:

$$\mathcal{O} \triangleq \begin{bmatrix} C \\ CA \\ \ldots \\ CA^{n-1} \end{bmatrix}$$

has rank n (full column rank).

The main advantage of using a state-space realisation is that it is more suitable for numerical calculations.

3.1.1 The $\mathcal{H}_\infty$ norm

If $G(s)$ is a stable scaler transfer function the $\mathcal{H}_\infty$ norm is the peak value of $|G(i\omega)|$ as a function of frequency:

$$\|G(s)\|_\infty \triangleq \max_\omega |G(i\omega)|$$

*Strictly speaking, "*max*" should be replaced by "*sup*" (the supremum, the least upper bound). The maximum may only be approached as $\omega \to \infty$ and may not actually be achieved. However, there is no difference between "*max*" and "*sup*" for engineering aims.* The system G(s) is stable if all poles (the roots of the input $u(s)$) or singularities of the transfer function have negative real part.

The symbol $\mathcal{H}$ stands for "Hardy space", a vector space. The $\mathcal{H}_\infty$ norm, being a very appropriate way of specifying both the amount of system uncertainty and signal gains in a closed-loop system, is a key measure of magnitudes in control and systems theory. The $\mathcal{H}_\infty$ control theory, consequently, is developed as a norm-based multivariable control design method, which deals with the $\mathcal{H}_\infty$ norms of the transfer functions in question.

Maybe it becomes clearer if first is explained where the symbol ∞ originates from. This symbol comes from the fact that the maximum magnitude over frequency may be written as:

$$\max_\omega |G(i\omega)| = \lim_{p\to\infty} \left(\int_{-\infty}^{\infty} |G(i\omega)|^p d\omega\right)^{1/p}$$

When $|G|$ is raised to an infinite power its peak value is picked out.

An important interpretation of the $\mathcal{H}_\infty$ norm can be given, if $G(s)$ is stable a linear single-input single-output system:

$$\|G(s)\|_\infty = \max_{\Re e\{s\}>0} \overline{\sigma}(G(s)) = \max_{\omega \epsilon \mathbb{R}} \overline{\sigma}(G(i\omega)) = \max_{u \neq 0} \frac{\|Gu\|_2}{\|u\|_2},$$

where $\|.\|_2$ is known as the bounded Euclidean norm, the shortest distance between two points. The maximum singular value, $\overline{\sigma}$ is frequency dependent and is extensively manipulated in $\mathcal{H}_\infty$ control design to meet the desired performance objectives. This is done by putting weights on signals entering and leaving the control configuration.

3.1.2 Formulation of a control problem

The standard $\mathcal{H}_\infty$ control problem is defined via the block diagram of Figure 3.2. This approach is useful when synthesising a controller.

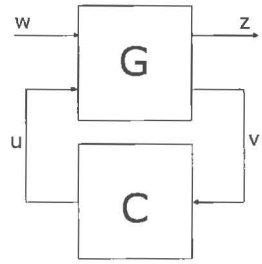

Figure 3.2: *General control configuration*

Here, G represents the general system, which includes the dynamics of a physical system along with the dynamics of all actuators, sensors and the weighting functions chosen to guarantee a desired performance; w contains the exogenous inputs to the system, such as disturbance signals, measurement noise, and reference inputs; z contains the outputs to be regulated; v is the measurement available for the feedback controller; and u is the control command signal from the controller. The standard optimal $\mathcal{H}_\infty$ control synthesis problem is then given as follows:

Design a feedback controller C which based on the information in v, generates a control signal u which counteracts the influence of w on z, thereby minimising the $\mathcal{H}_\infty$ norm of the closed-loop transfer function from w to z

The closed-loop transfer function from w to z is named T_{zw}. The minimum value of $\|T_{\mathrm{zw}}\|_\infty$ is called the *optimal performance*, and is usually denoted by γ_{opt}. Instead of minimising the $\mathcal{H}_\infty$ norm of T_{zw}, if it is desired to be made smaller than a prespecified $\gamma > \gamma_{\mathrm{opt}}$, then the new problem is called the *suboptimal $\mathcal{H}_\infty$ problem.* Note that, although γ is referred to as optimal or suboptimal performance, it is more like a cost measure rather than a performance measure, i.e. γ is a quantity that is desired to be small like a cost, rather than some performance measure which is desired to be large.

The system of Figure 3.2 is described by:

$$\begin{bmatrix} z \\ v \end{bmatrix} = G(s) \begin{bmatrix} w \\ u \end{bmatrix}$$

$$u = C(s)v$$

The feedback system represented in Figure 3.3 can be transformed in the general control configuration shown in Figure 3.4. The first step is to identify the signals for the general plant:

$$w = \begin{bmatrix} w_1 \\ w_2 \\ w_3 \end{bmatrix} = \begin{bmatrix} r \\ d \\ \eta \end{bmatrix};$$

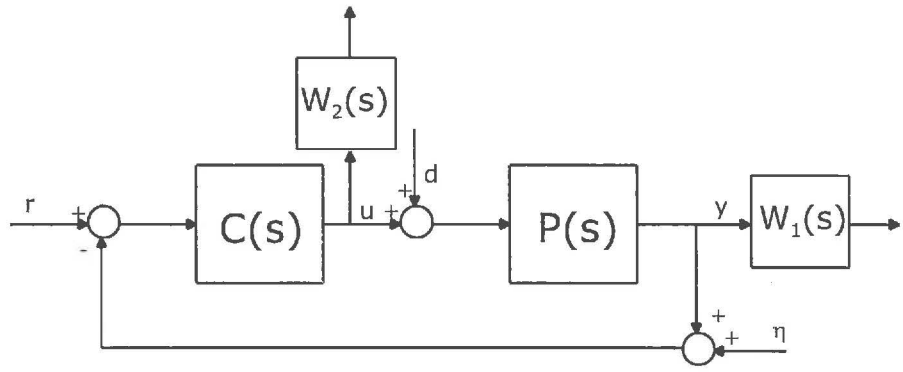

Figure 3.3: *feedback control configuration*

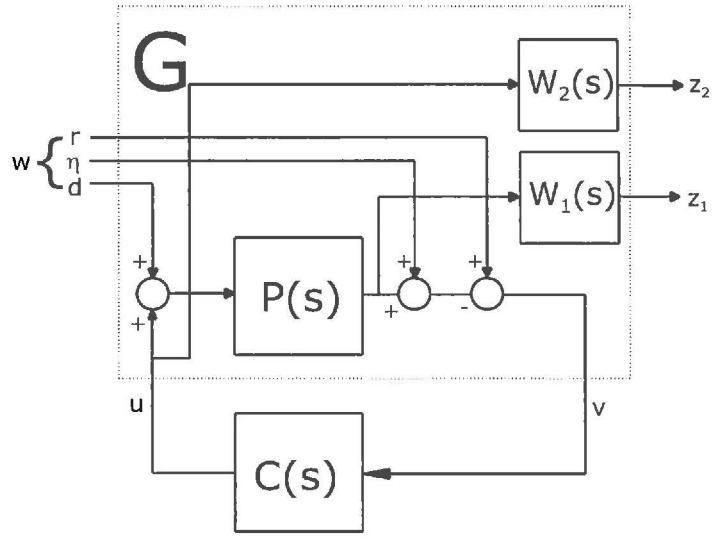

Figure 3.4: *Equivalent representation of Figure 3.3*

$$z = \begin{bmatrix} z_1 \\ z_2 \end{bmatrix} = \begin{bmatrix} W_1(s)y \\ W_2(s)u \end{bmatrix};$$
$$v = r - (y + \eta),$$

where r is the reference input, d is the disturbance and η the measurement noise. $W_1(s)$ and $W_2(s)$ are weighting filters, assumed to be stable and minimum phase. Minimum phase systems do not have time delays or right-half plane zeros. The block diagram in Figure 3.4 yields:

$$z_1 = W_1(s)y = W_1(Pd + Pu) = W_1(s)P(s)w_2 + W_1(s)P(s)u$$

$$v = r - y - \eta = r - P(s)d - P(s)u - \eta = Iw_1 - P(s)w_2 - Iw_3 - P(s)u$$

and G which represents the transfer function matrix from $\begin{bmatrix} w & u \end{bmatrix}^T$ to $\begin{bmatrix} z & v \end{bmatrix}^T$ is:

$$G(s) = \begin{bmatrix} 0 & W_1(s)P(s) & 0 & W_1(s)P(s) \\ 0 & 0 & 0 & W_2(s) \\ I & -P(s) & -I & -P(s) \end{bmatrix}$$

Alternatively, G can be obtained from the representation in Figure 3.3. The state-space realisation is derived in appendix B.

3.2 $\mathcal{H}_\infty$ control for flame instabilities

In chapter 2 the following model describing the flame dynamics has been derived:

$$P(s) = \frac{Q(s)}{U(s)} = \frac{\rho_u c_p(\overline{T}_b - \overline{T}_u)}{\frac{\tau_f}{Z} s \exp(s\frac{\psi_f}{\overline{u}_u}) + 1}, \tag{3.3}$$

Before a controller can be synthesised, first the stability of the system is investigated using D-partition. The stability depend on the place of the poles. If all poles are located in the left-half plane of the s-plane, the system is stable. A delay-differential equation has infinite number of poles. All these poles should lie in the left-half of the complex plane for a stable system.

The flame dynamics is expressed by:

$$\dot{q}(\tau) + \frac{Z}{\tau_f} q(\tau') = \frac{Z}{\tau_f} \frac{\rho_u}{c_p(\overline{T}_b - \overline{T}_u)} u(\tau'),$$

with with $\tau' = \tau - \psi_f/\overline{u}_u$, the delayed time. In the Laplace domain the system becomes:

$$(s + \frac{Z}{\tau_f} \exp(-s\frac{\psi_f}{\overline{u}_u}))Q(s) = \frac{Z}{\tau_f} \frac{\rho_u}{c_p(\overline{T}_b - \overline{T}_u)} \exp(-s\frac{\psi_f}{\overline{u}_u})U(s)$$

The characteristic equation of this system can be described as:

$$s + \frac{Z}{\tau_f} \exp(-s\frac{\psi_f}{\overline{u}_u}) = 0$$

Introducing the parameters $S = s(\psi_f/\overline{u}_u)$ and $\xi = (Z/\tau_f)(\psi_f/\overline{u}_u)$, the characteristic equation can be expressed in terms of a single parameter ξ:

$$S + \xi \exp(-S) = 0$$

This equation can be solved for ξ:

$$\xi = -S \exp(S)$$

The values of ξ, corresponding to the imaginary axis of the s-plane are given by:

$$\xi(\omega) = -i\omega \exp(i\omega) = \omega \sin(\omega) - i\omega \cos(\omega), \qquad -\infty < \omega < +\infty$$

In Figure 3.5, the D-partition diagram is shown for this system. The domain which contains the segment $0 < \xi < pi/2$ of the real axis, is the domain where the number of poles with a positive real part has its minimum, in this case zero.

The parameter space can be divided into domains $D(k, n-k)$, $0 \leq k \leq n$, which contains all the points with poles with k negative real parts and $n-k$ positive real parts. This is called D-partitioning. The domain of asymptotic stability is the domain $D(n, 0)$. An increase of the number of roots with positive real parts can only occur if a certain pole crosses the imaginary axis from the left to the right. This corresponds with a move from the domain $D(k, n-k)$ to $D(k-1, n-(k-1))$. Therefore the borders of the D-partitions are the map of the imaginary axis $s = i\omega$, $-\infty < \omega < +\infty$ on the s-plane.

With the values imposed by the operating point ($\Phi = 0.8$ and $\overline{u}_u = 0.14$cm/s the poles are located in the stable region D(0).

3.2.1 Time delay

Because the algorithms in Matlab for synthesising a controller require a state-space realisation of the model a technique to cope with the time delay has to be found. Regarding the controller design phase, three general approaches are possible.

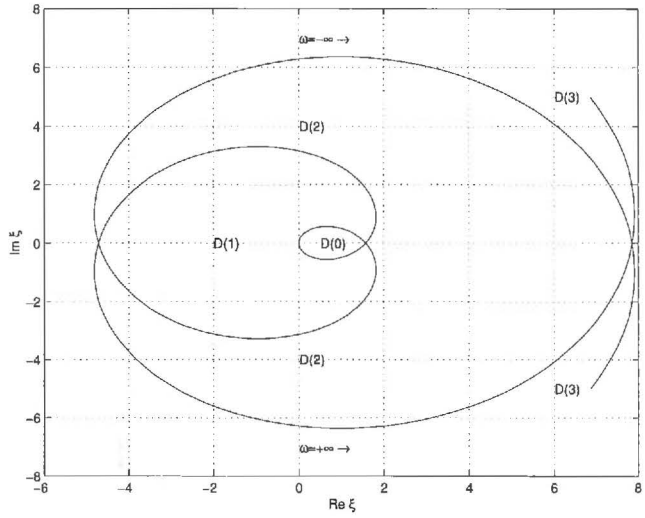

Figure 3.5: *D-partition diagram. D(0) is the domain where the number of roots with positive real part is zero*

- *Classical Control* When taking a look at the transfer function of the system derived in chapter 2, the time delay is indicated by $\psi_f/\overline{u}_u$. The problem with the time delay can be reduced to a conventional one by expressing the non rational function $-\exp(\frac{\psi_f}{u_u}s)$ in terms of a rational function. Note that the function $-\exp(\frac{\psi_f}{u_u}s)$ is analytic (for finite values of s), so the approximation is allowed. A typical approach is to use the Padé approximant. The value of this method is limited by two factors. First the rational approximation of the delay rapid increases the effective order of the system, making the control design problematic. Second, large value of time delay will decrease the available phase margin to the point where it is no longer possible to design a stabilising controller.

- *Modern Control* Dead time is in this case viewed as an uncertainty in the system and is incorporated in the design as a perturbation to the original system;

- *Delay Compensation* This category includes all the other methods used for time delay. An important group include compensation networks that bring the delay 'out of the loop', and hence allow to design the controller using conventional methods applied to the system without time delay. An example is the Smith Regulator. A caveat here is constituted by the fact that the most networks based on linear elements generally do not modify the eigenvalues of the original system, so they only apply to stable (or marginally stable) systems. On the other hand, arbitrarily large time delays can be accounted for without loss of stability margin.

Here the first approach, *Classical Control* will be used. The Padé approximation is described by:

$$\exp(-sT) = 1 - sT + \frac{1}{2!}(sT)^2 + ...$$

A sixth order Padé approximation for a time delay of 2.6 ms is used. The approximated transfer function becomes then a seventh order model. In Figure 3.6 can be seen that the approximation is nearly perfect. The straight line is the original transfer function and the dotted line is the approximation of this transfer function.

Figure 3.7 shows the location of the poles and zeros of the approximated transfer function. It can be seen that two poles are situated in the right-half plane.$(28.3 \pm 613i)$ As a result of this the approximation is not stable.

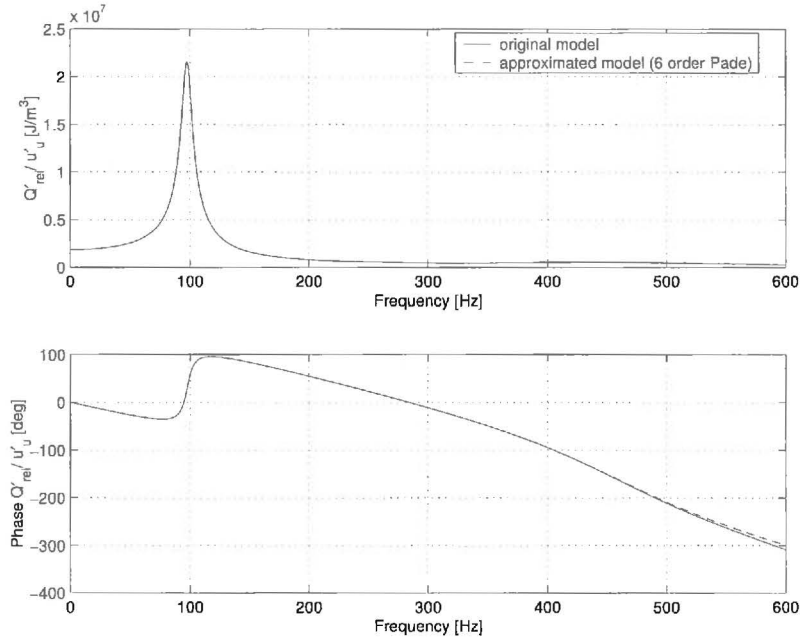

Figure 3.6: *Comparison of rational approximation to P(s) over the frequency range of interest*

3.2.2 Stabilising the system

Controller design are usually easier to solve when the system to be controlled is stable a two-stage controller design is chosen. This is shown in Figure 3.8

The first stage is used to stabilise the system and the second stage is used to achieve the performance criteria. The important fact in doing a two-stage design is that one can always stabilise the closed-loop. However, not all controllers, stabilising a certain system can be realised by a two-stage design. This is possible if and only of the inner-loop controller $C_1(s)$ is stable.

For the inner-loop the following relation can be derived:

$$H(s) = \frac{C_1(s)}{1 + C_1(s)P_{r(s)}}, \tag{3.4}$$

with $P_r(s)$ the approximation for $P(s)$. The Routh-Hurwitz stability criterion will be used to synthesise the controller $C_1(s)$. This criterion is a necessary and sufficient criterion for the stability of linear systems. It determines stability by examining the characteristic equation of the transfer function $H(s)$. The criterion states that the number of roots with positive real parts is equal to the number of changes of sign in the Routh array.[Dor95] The Routh array is a way of ordering the the coefficients of the characteristic equation. The characteristic equation for the transfer function in (3.4) is given by:

$$q(s) = 1 + C_1(s)P_r(s)$$

$C_1(s)$ is free to choose. Here a proportional controller is used to set the closed-loop roots of $1 + C_1(s)P_r(s) = 0$ at desired positions and then solve for the gain value of $C_1(s)$ that is required. The roots have to be located in the left-half plane. This can be done with a gain of $1 \cdot 10^{-8}$. Figure 3.9 shows the locations of the poles (closed-loop roots) and zeros of the transfer function $H(s)$

3.2.3 Second-stage design

Figure 3.10 represents the performance problem, minimising the effect of the fluctuations in gas velocity, d, on the total heat release y. An extra input θ is used, that represents unknown disturbances caused by for instance the geometry of the burner.

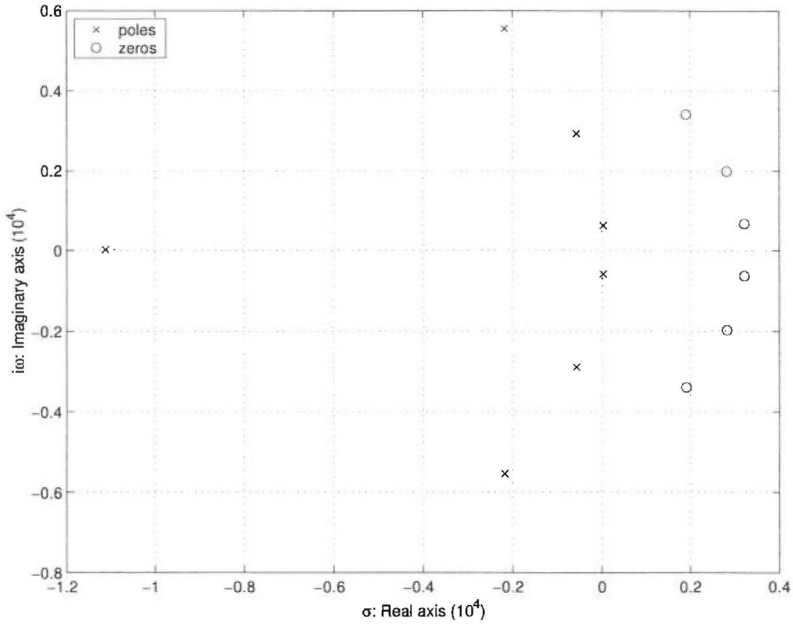

Figure 3.7: *Root Locus: locations of the poles(x) and zeros(o)*

The transfer function matrix for his problem can be derived with the method shown above:

$$G(s) = \begin{bmatrix} W_1(s)H(s) & W_1(s)H(s) & W_1(s)H(s) \\ 0 & 0 & W_2(s) \\ -H(s) & -H(s) & -H(s) \end{bmatrix},$$

with $w = [d \quad q]^T$ and $z = [W_1(s)y \quad W_2(s)u]^T$ and $v = -y$. $W_1(s)$ and $W_2(s)$ are respectively the weights on the actuator signal u and the output y. Weights are a tool, that can help to reach the desired performance criteria.

The weight on y is modelled as a bandpass filter and shown in Figure 3.11, because our only interest is in low frequencies, $f \leq 600$ Hz. The bandpass filter is based on a second-order low-pass Butterworth filter. The weighting filter of u describes the dependency of the control signal on the characteristics of the actuator, here the weight is considered to be the identity. The major reason for this is that $\mathcal{H}_\infty$ control procedure does not provide a natural way to include time domain specifications suchas actuator saturation limits.

After checking the observability and controllability of $H(s)$ the second controller is synthesised using the γ-iteration of Safonov and Chiang, included in Matlab's robust control toolbox (*hinf.m*). This controller design algorithm is chosen over the well-known Glover-MacFarlane method for it simplicity. This algorithm is included in the μ-toolbox of Matlab (*hinfsyn.m*)

Figure 3.12 shows the results from simulation using Simulink. As input signals sinusoidal waves, with a frequency of 160 HZ are used for d with an amplitude of 0.5 cm/s and for θ with an amplitude of 5 cm/s. The controller suppresses the perturbation in heat release, this causes a reduction in fluctuations in gas velocity. A delay can be noticed in the figure, due to flame dynamics. It seems possible with a $\mathcal{H}_\infty$ controller to suppress instabilities. This will be evaluated during experiments in the next chapter.

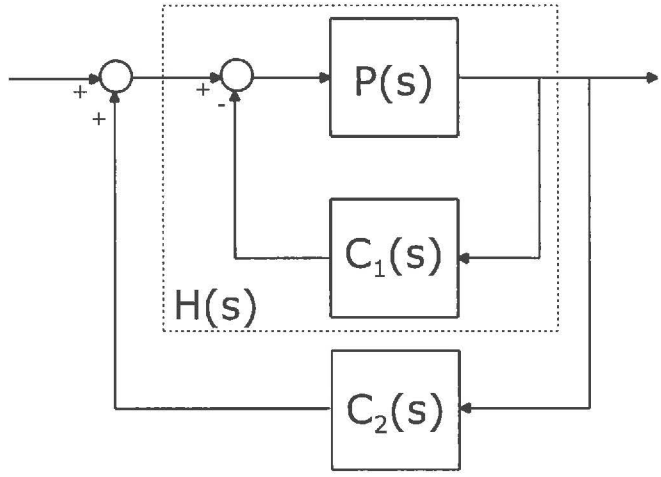

Figure 3.8: *Two-stage Controller*

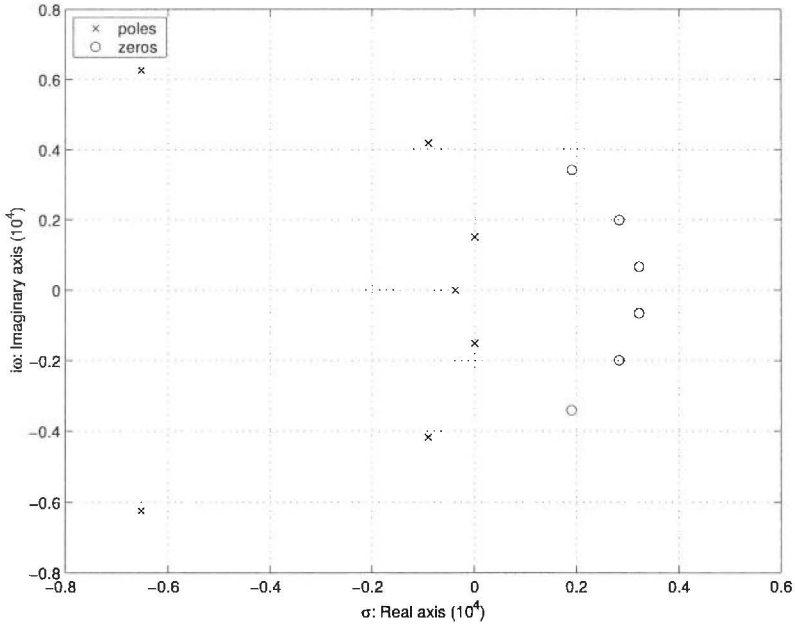

Figure 3.9: *Root Locus: locations of the poles(x) and zeros(o)*

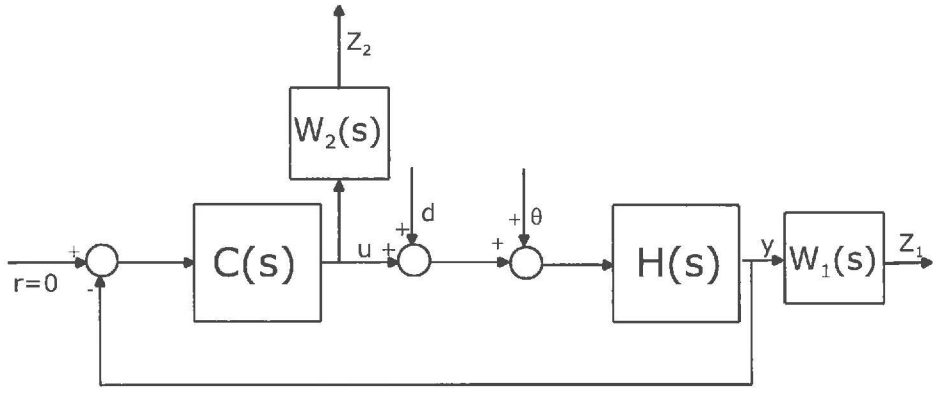

Figure 3.10: *Feedback control configuration*

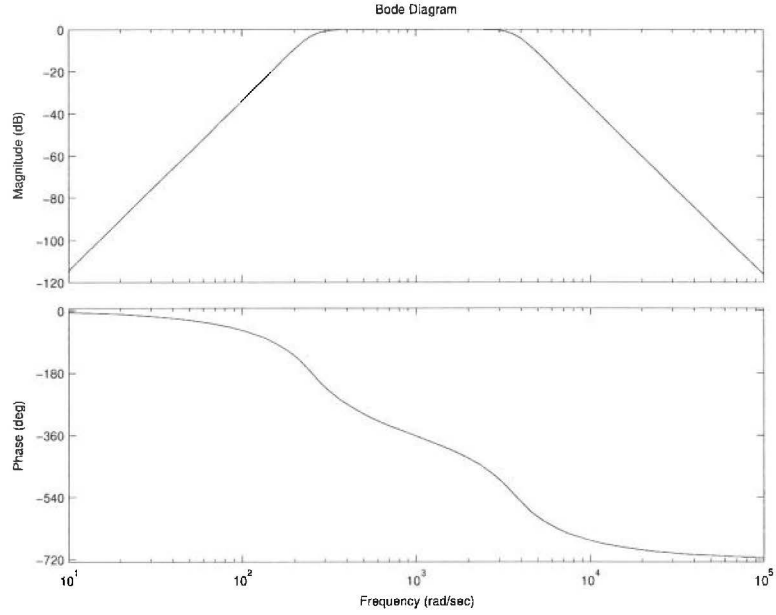

Figure 3.11: *Bode Diagram, representing the weighting filter* $W_1(s)$

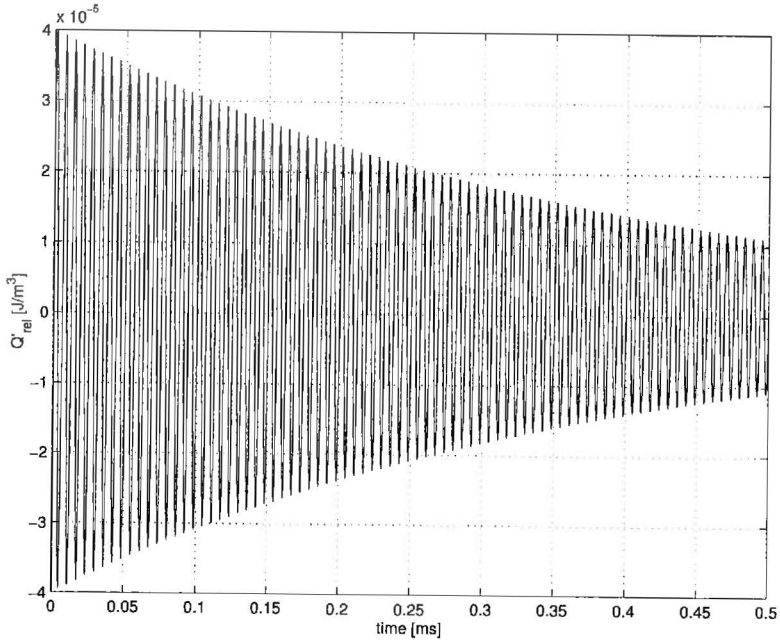

Figure 3.12: *Controlled Heat-release*

Chapter 4

Experimental testing

In this chapter, the previously developed $\mathcal{H}_\infty$ controller will be tested during an experiment. The configuration considered consists of a laminar premixed flame on a flat surface burner. The combustion system is excited/actuated by an external source. After a description of the measurement methods and system identification the performance of the controller implemented for feedback control will be examined.

4.1 The experimental set-up

A vertical cylindrical tube of 500 mm length and 50 mm diameter, open at one end is considered and shown in Figures 4.1 and 4.2. The tube is closed at the bottom with a flange. Through a small hole in the flange the premixed methane/air mixture enters the tube. This flow is settled by the use of grids right after the inlet. Near the bottom of the tube an opening is made in the side. This opening is coupled by a flexible hose to a loudspeaker. This speaker is used to excite the system. In order to apply active control to the system, the actuator, also a loudspeaker, is situated before the inlet of the tube. This speaker is coupled using a branch pipe with the flow. To allow the gas to escape the tube is open at the top. The burner plate is placed approximately 75 mm below the exit. This was done to avoid problems with the determination of the velocity fluctuations. An open end will in general act as a perfect reflector of acoustic waves, causing a maximum of the velocity fluctuations at the open end. [Roo01] The burner plate and the part of the tube downstream (the region after the burner plate) of the burner plate are cooled at nominally 323 K. The plate is a perforated brass disk with a thickness of 2 mm. The perforation pattern is hexagonal, with a hole diameter of 0.5 mm and a distance of 0.7 mm between the holes. The opening size is small enough that a premixed methane/air flame stabilises on top of it.

To allow for the use of the two-microphone method, a manner to measure the velocity in the flow, two pressure transducers are mounted at different heights in the side of the tube. Optical access in the downstream region is needed to make it possible to measure the velocity using laser Doppler velocimetry. Therefore three openings have been made in the downstream part. Two holes serve as an entrance for the laser beams and through the third one the scattered light is captured by a photo-multiplier. Another photo-multiplier is mounted at a distance of 500 mm above the burner plate and is used for heat-release measurements based on chemiluminescence.

The performance of the controller will be judged on the amount of suppression of velocity fluctuations downstream of the burner deck.

4.1.1 Two-microphone method

To be able to measure the velocity fluctuations just below the burner deck two pressure transducers are mounted at different positions (113 mm and 383 mm below the burner deck) in the tube. The velocity can be determined, from the ratio between a (fixed) distance and a time difference. This

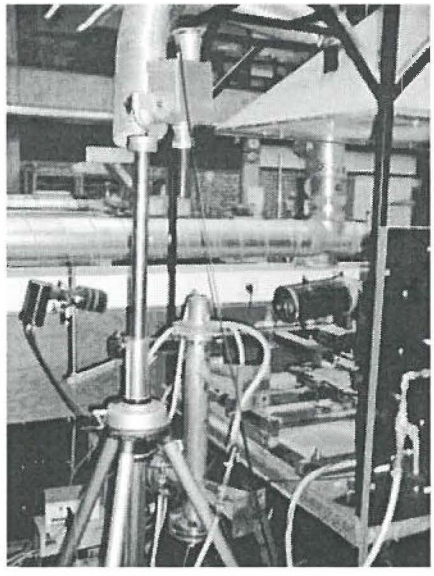

Figure 4.1: *Photograph of the experimental setup*

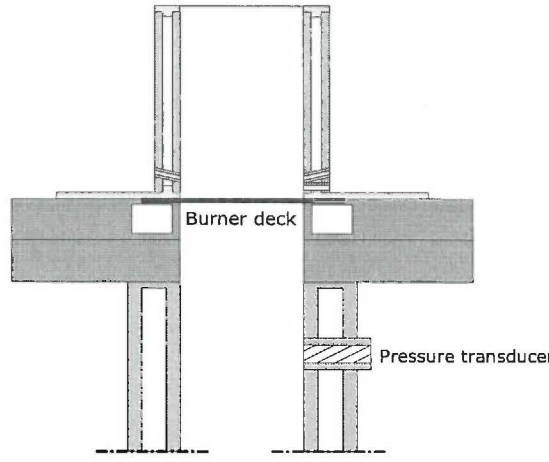

Figure 4.2: *sketch of burner head*

difference is caused by the fact that the flow reaches the transducers at a different time. This is a standard technique, more details can be found in Munjal [Mun87].

4.1.2 Laser Doppler velicometry

Laser Doppler velocimetry (LDV), also called anemometry, is a manner of measuring velocities downstream of the burner deck. It's non-intrusive principle and directional sensitivity make it very suitable for applications with reversing flow, chemically reacting or high-temperature media and rotating machinery, where physical sensors are difficult or impossible to use. Ideally, the particles should be small enough to follow the flow, yet large enough to scatter sufficient light to obtain a good signal-to-noise ratio at the photo-detector output.

Flow velocity information comes from light scattered by tiny "seeding" particles carried in the fluid as they move through the probe volume. The scattered light contains a Doppler shift, which is proportional to the velocity component perpendicular to the bisector of the two laser beams.

The scattered light is collected by a receiver lens and focused on a photo-detector. An interference filter mounted before the photo-detector passes only the required wavelength to the photo-detector. This removes noise from ambient light and from other wavelengths. More details can be found in Steenhoven *et al.* [Ste01].

4.1.3 Chemiluminescence

A real-time measurement of the velocity fluctuations downstream of the burner can be performed using chemiluminescence. Chemiluminescence is the generation of electromagnetic radiation as light by the release of energy from a chemical reaction. While the light can, in principle, be emitted in the ultraviolet, visible or infrared region, those emitting visible light are the most common.

Chemiluminescence of flames is especially interesting because the concentrations of excited molecules seen in flames exceed the equilibrium concentrations expected at the same temperature without chemical reaction by several orders of magnitude. It is possible to deduce from this fact that excited molecules are not only produced by thermal excitation but also are produced as the products of reactions. Since the amount of radiation observed in the flame at a particular wavelength is proportional to the concentration of the associated excited molecule, a measurement of the radiation can be directly related to the concentration of the excited molecule.

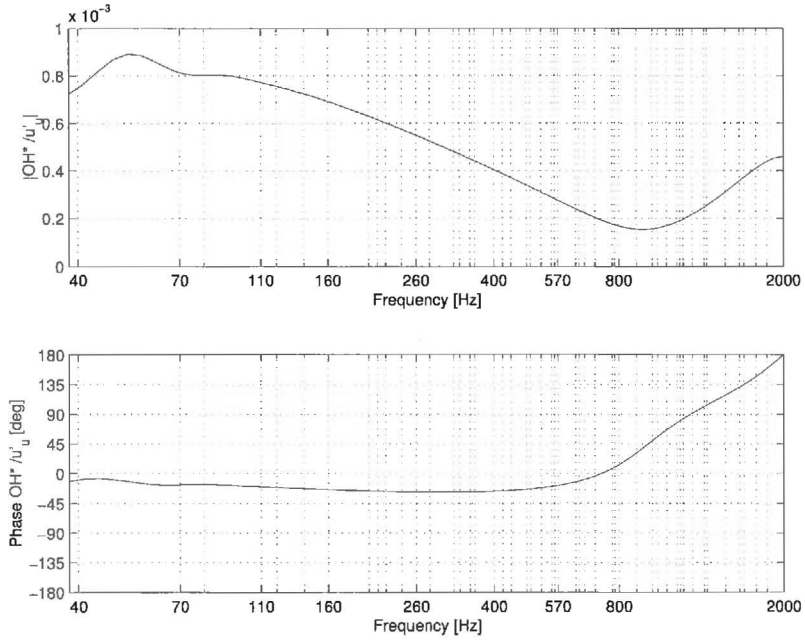

Figure 4.3: *Frequency response of OH* production rate*

The concentration of OH∗ molecules is supposed to be a quantitative measure for the heat release. The ∗ denotes the excited molecule. OH∗ molecules emit light with a wavelength of 308 nm. (ultraviolet)

In general a linear relation between the heat-release Q_{rel} and the concentration of OH∗ is assumed, this is also supported by Figure 4.3. This is the result of a numerical simulation using *Chem1D*. In a quasi-stationair regime this means:

$$Q' = kE',$$

where k is a constant and E is the production rate of OH∗.

4.1.4 Remarks on the choice of a sensor and actuator

The most commonly used sensor for active instability control is a pressure transducer. Unfortunately the two-microphone method only suffices to characterise the velocity of the medium if the medium has constant properties (density and temperature)[Mun87]. This is only valid in the upstream region of the flame.

The measurements done with LDV have to be evaluated before they can be used as an input signal for the controller. Therefore the light emitted by OH radicals in the flame is used as the input to the controller. This signal has one major disadvantage. It is very sensitive to noise, for instance the UV emitted by fluorescent lights can be noticed very well(50 Hz). All measurements are for that reason preformed with the lights turned off.

In laboratory scale experiments hot wire anemometry has been used to measure the fluctuating heat-release, but this method will not sufficiently be robust in a practical combustion system. Maybe a more robust and reliable instantaneous measurement of velocity could be provided in the future (the use of Micro-electro Mechanical Systems seems a promising technique), and used as an input to the controller.

Another possibility could be the use of an ionisation probe. But caution have to be paid, when using this method, this is observed when try to implement this method on the test-rig.

The most convenient method is to use a loudspeaker as an actuator to cancel the disturbances. Another possibility is to change the equivalence ratio. This has to be carried out with precaution. Therefore the most obvious method is chosen.

4.2 System identification

The measured model, a transfer function between velocity fluctuations upstream and heat-release downstream of the burner deck is shown in Figure ??. The inverse of the model derived in chapter 2 is fitted on this transfer function using a (weighted) least-square fit.

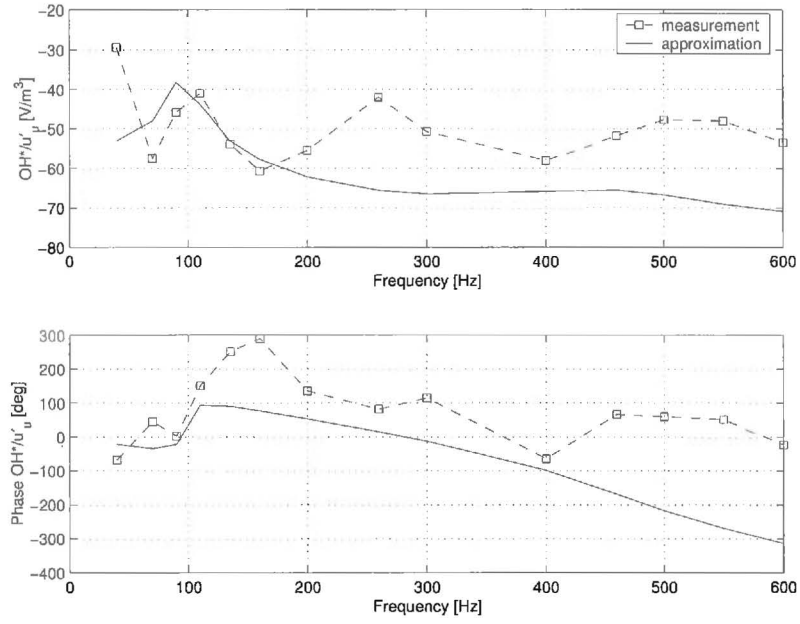

Figure 4.4: *Transfer function of the measured OH*emmission and velocity fluctuation*

The objective of parameter optimisation (estimation) is to find the parameter vector $\theta \in \mathbb{R}^n$ of a model which minimises a chosen measure of the output error. The output error is defined as

$$e_i(\theta) = y_i - \hat{y}_i(\theta),$$

where $\{\hat{y}_i\}_{i=1}^N$ is the model output sequence, and $\{y_i\}_{i=1}^N$ is the desired model response sequence; N denotes the number of data points. The weighted sum of the squared output error will be used in the formulation of optimisation criterion,

$$J(\theta) = f[e_i(\theta)] = \sum_{i=1}^{N} \gamma_i [y_i - \hat{y}_i(\theta)]^2,$$

where γ_i are the weighting factors for each data point. The weighting factors are chosen to be equal to 1, because it is not clear what a right choice for the weights would be . The following values are found $\frac{Z}{\tau_f} = 700$, $\rho_u c_p(\overline{T}_b - \overline{T}_u) = 2466$, $k = 1 * 10^{-8}$ and the time delay is 2.5 ms. More details on system identification can be found in Ljung [Lju87].

4.3 Implementation of the controller

The experimental setup is schematically shown in Figure (4.5).

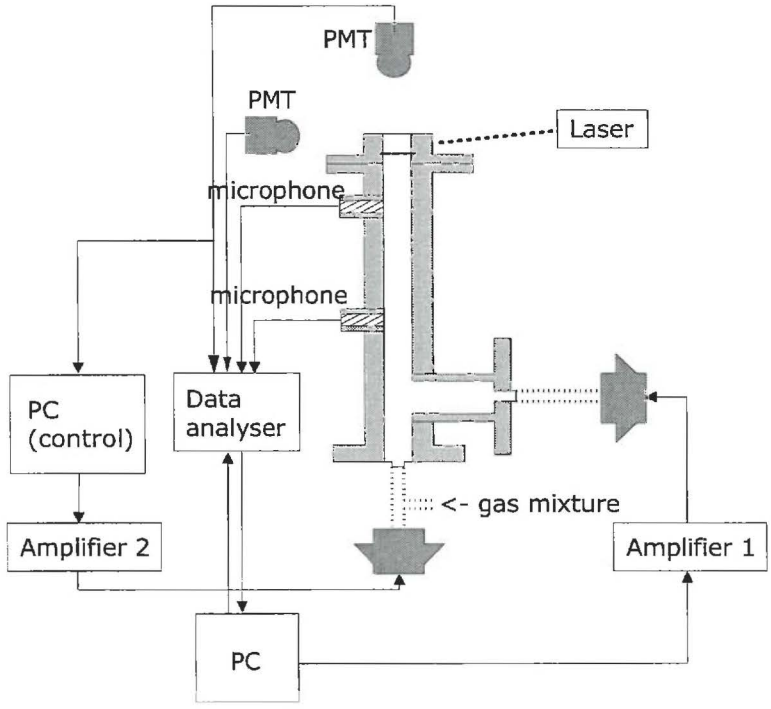

Figure 4.5: *Schematic representation of the experimental setup*

The composition of the premixed mixture (methane and air) is controlled using mass-flow controllers. The mixture is lighted at the open end of the tube. The data acquisition system (HP spectrum analyser) and a Personal Computer are responsible for collecting and storing most of the relevant info of the experiments. The data acquisition system takes incoming data and then writes the data to formatted files for pos-processing and further evaluation. The data acquisition system is not PC-based. The hardware changes, because there are only 4 inputs, and the software driving the data analyser is the same in all cases. The first input is connected to the reference wave (needed for evaluation), input 2 and 3 are the signals of the pressure transducers and input 4 is signal from the LDV or the Chemiluminescence. The reference wave (a sinusoidal wave, the frequency can be changed) is generated by the software of the data-analyser and sent via a amplifier (Cyrus III) to a loudspeaker (Monocor KU-100). Through this speaker a oscillation is applied in the tube.

For control purposes an extra computer is needed. This computer is equipped with a NIA PCI AT-MIO-16-XE-10 (a multifunction DAQ board), combined with an shielded I/O Connector Block (SCB-68). The disadvantage of this DAQ board is that has no own processor. For that reason to connect this board to Simulink is not as convenient as with a dSpace system (often used in the DCT laboratory). Luckily Matlab has a tool, called Real-Time Windows Target, which makes the connection between Simulink and the DAQ board possible. The state-space representation of the controller represented by a block in Simulink is transformed into 'C++'-code (by the Real-Time Workshop). The controller characteristics can then be overtaken by the acquisition board. As an input to the DAQ board the signal of the PMT, measuring the chemiluminescence, is used. The output is connected to a different amplifier which introduces via an other loudspeaker an oscillation in the system. This oscillation is used to cancel the first one.

To test if it is really possible to suppress flame instabilities a phase-delay controller is used. This controller consists of a gain and a time delay. Figure 4.6 shows the results for the first controller. The oscillation is driven by a sine wave of 160Hz. The gain of the phase-delay controller is set to 1 and the delay to 0.0055s. The flame is burning in a linear regime. (During all experiments

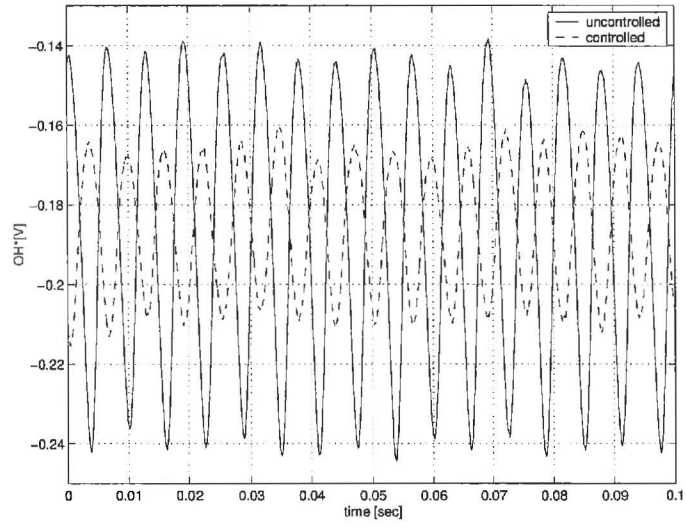

Figure 4.6: Response of OH*-signal in uncontrolled and controlled situation

a Φ of 0.8 and a $\overline{u}_u$ of 14 cm/s is used.) The magnitude of the quotient u'_b/u'_u, measured using LDV, is almost three times smaller. (2.25 instead of 6.3±0.5). For every different driving signal (reference) a new phase-lag controller has to be derived. That is why no more attention is paid to this controller and experiments have been started with the $\mathcal{H}_\infty$ controller.

Implementation of the $\mathcal{H}_\infty$ controller has not been easy. There were problems with the second loudspeaker, the power of the signal was too weak (maybe through bad incoupling) and it seems that there is a phase dependency between both speakers. (This need more investigation.) The delivery of a new Monocor KU-100 lasted several weeks, so new measurements have not been performed yet, with a powerful loudspeaker.

Secondly when the $\mathcal{H}_\infty$ controller worked, the system became unstable after several seconds. The controller is not albe to stabilise the system again. This is probably caused through the linear model. The fluctuations in heat-release are too big, so description of the system may not be linearised. An approach based on limit-cycles could give a better result.

4.4 Conclusion

It is possible to suppress flame instabilities using feedback control, see Figure 4.6. This is not a model-based approach and not all performance criteria stated in Chapter 1 are fulfilled. It seems that the $\mathcal{H}_\infty$ controller does not perform as expected. The precise cause has not yet been identified, maybe its the model, or the implementation of the controller, therefore, more research is needed.

Chapter 5

Conclusions and recommendations

5.1 Conclusions

Modern central-heating boilers, equipped with fully premixed surface burners, are sensitive to combustion instabilities. These self-excited combustion oscillations result from a coupling between unsteady heat-release and acoustic waves within the combustor. The goal of this work is to investigate if it is possible to suppress combustion oscillations of premixed flames stabilised on a flat surface burner using a closed-loop control strategy.

After a short introduction on the Rayleigh criterion a model for the fluctuating mass burning rate based on the G-equation is derived. This model is then used to derive a linearised model for the relation between fluctuating heat-release and gas velocity (flame dynamics)

The controller is synthesised using a model-based technique, namely $\mathcal{H}_\infty$. This is justified by the control problem under investigation. The effect of disturbances in heat-release, caused by acoustic waves, has to be minimised, a typical performance problem. Before the design of the controller could take place the model is written in a state-space realisation. Unfortunately the linearised model contains a time delay. This delay is approximated by a sixth order Padé approximation. This resulted in an unstable system. No $\mathcal{H}_\infty$ algorithm part of Matlab is able to synthesise a controller, that makes the closed-loop system stable. Therefore a proportional stabilising controller is derived using Routh-Hurwitz method. This controller along with the flame dynamics becomes then the new system under investigation. Now it is possible to synthesise a controller that suppress the instabilities and guarantee closed-loop stability.

After simulations using Simulink and the introduction of the measurement methods feedback control is tested experimentally. During experiments sinusoidal disturbances (acoustic wave) with changing frequency are used. First a phase-lag controller, consisting of proportional gain and a time delay is implemented. This type of controller performs his job quite well. The great disadvantage is that for every frequency of the disturbance a new controller has to be found empirically. The power of $\mathcal{H}_\infty$ control is that it has to be capable of dealing with a range of frequencies. Unfortunately the implementation of this controller caused problems, it seems to work for a few seconds, but the system becomes unstable, resulting in an amplification of the disturbances. A possible explanation is found in the fact that the model is linearised at a equivalence ratio of 0.8 and a gas velcoity of 14 cm/s. The fluctuations in heat-release may be too big, thus a linearisation is not allowed. Furthermore the derived model is arbitrarily chosen. The relation between heat-release and chemiluminescence is assumed to be linear. Another reason could be the fact that we use two loudspeakers in the experiment. The signal of one speaker is used to disturb the flame and the other speaker is used to cancel this disturbance. The phase relation between both loudspeakers has to be optimal to get good disturbance attenuation. Maybe it would be easier if a self-exciting system, like a Rijke tube, had been used to test the control strategy.

5.2 Recommendations

- There are several manners to make a model of a system, for instance identification of the transfer function experimentally, or based on the conservation equation of mass, species mass fractions, energy and momentum, for example the model of Rook [Roo01]. If the latter is used then research has to be done how to control fractional systems. Fractional systems are systems containing $\sqrt{s}$ in the transfer function. A possible solution is to use polynomial approximations or the method described in Loiseau *et al.* [Loi98]. In their paper a heat transfer problem (one-dimensional heat conducting rod) is controlled based on classical control techniques;

- In the end a controller is needed that suppress self-excited oscillations. Therefore, the synthesised controller has to be tested in a self-exciting system. This can easily be done if the tube is extended in length. The system behaves then as a Rijke tube. An advantage is that no phase relation will exist between the disturbance and the control signal;

- The experiments were performed with a mixture of methane and air. Normally a central-heating boiler is fed with natural gas, containing also a little bit of propane and ethane. The composition of the natural gas differs day by day. Research is needed if the controller is robust with respect to changes in gas composition.

Bibliography

[Ana02] Annaswamy, A.M. & Ghoniem, A.F., *Active Control of Combustion Instability: Theory and Practice*, IEEE Control Systems Magazine, December 2002, pp. 37-54 (2002). [article]

[Cam03] Campos-Delgado, D.U., Schuermans, B.B.H., Zhou, K., Paschereit, C.O., Gallestey, E.A. & Poncet, A., *Thermoacoustic Instabilities: Modeling and Control*, IEEE Transactions on Control Systems Technology, vol. 11, no. 4, pp. 429-447 (2003). [article]

[Dor95] Dorf, R.C. & Bishop R.H., *Modern Control Systems, 7th edition*, Addison-Wesley Publishing Company, Inc., Reading, Massachusetts (1995). [book]

[Dow83] Dowling A.P. & Ffowcs Williams J.E., *Sound and Sources of Sound*, Ellis Horwood Limited, Chichester (1983). [book]

[Dow99] Dowling, A.P., *A kinematic model of a ducted flame*, Journal of Fluid Mechanics, vol. 394, pp. 51-72 (1999). [article]

[Eve03] Evesque, S., Dowling, A.P. & Annaswamy, A.M., *Self-tuning regulators for combustion oscillations*, to appear in Proceedings Royal Society, London (2003). [article]

[FLe96] Fleifil, M., Annaswamy, A.M., Ghoniem, Z.A., & Ghoniem, A.F., *Response of a Laminar Premixed Flame to Flow Oscillations: A kinematic Model of Thermoacoustic Instability Results*, Combustion and Flame, vol. 106, pp. 487-510 (1996). [article]

[Goe03] *private communications with Prof. Dr. L.P.H. de Goey* (2003)

[Jan02] Janssen, R.W.M. *The effect of heat transfer on acoustics in burner-stabilised flat flames*, Eindhoven University Press (2002). [report]

[Lan90] Langhorne, P., Dowling, A.P. & Hooper, N., *Practical active control system for combustion oscillations*, Journal of Propulsion and Power, vol. 6, pp. 324-330 (1990). [article]

[Lju87] Ljung, L., *System identification: Theory for the user*, Prentice Hall, Englewood Cliff (1987). [book]

[Lui98] Loiseau, J.J. & Mounier, H., *Stabilisation de l'équation de la chaleur commandée en flux*, ESIAM Proceedings, vol. 5, pp. 131-144 (1998). [article]

[Mun87] Munjal, M.L., *Acoustics of ducts and mufflers*, John Wiley & Sons, Inc., New York (1987). [book]

[Poi87] Poinsot, T., Bourienne, F., Candel, S., Esposito, E. & Lang, W., *Suppression of combustion instabilities by active control*, Journal of Propulsion and Power, vol. 5, pp. 14-20 (1987). [article]

[Roo01] Rook, R., *Acoustics in Burner-Stabilised Flames*, Eindhoven University Press (2001). [book]

[Ste01] Steenhoven, A.A., & Schreel, K.R.A.M., *Fysische Meetmethoden*, Eindhoven University Press (2001). [book]

[Sko96] Skogestad, S., Postlethwaite, I., *Multivariable Feedback Control: Analysis and Design*, John Wiley & Sons, New York (1996). [book]

[Zho98] Zhou, K. with Doyle, J.C., *Essentials of Robust Control: International Edition*, Prentice-Hall International, London (1998). [book]

Appendix A

Acoustic Wave

The acoustic waves in Figure 2.1 are plane waves, because they can only transport acoustic energy. When plane waves of equal amplitude are travelling in opposite directions, they add in such a way as to produce a wave that oscillates in amplitude but does not move in space. Such a wave field is called a standing wave.

Standing waves are produced in any confined chamber, the amplitudes of which are functions of geometry, boundary conditions, and the medium. Often these pressure variations serve as a host oscillator in combustion system. Various pressure modes can be excited, such as bulk, longitudinal, azimuthal, or radial, the exact natures of which are determined primarily by the geometry of the combustor.

The general equation for acoustics can be derived as:

$$\frac{\partial e'}{\partial t} + \nabla \cdot E' = G(x,t), \tag{A.1}$$

where e' is the generalised acoustic energy density, E' is the generalised acoustic energy flux, and $G(x,t)$ represents excitation effects, including unsteadiness in heat and mass addition, entropy fluctuations, and vorticity fluctuations [Ana02].

Using the predominantly one-dimensional configurations typically present in combustors, equation (A.1) can be simplified further. The equation for a longitudinal geometry are given by:

$$\frac{\partial^2 p'(x,t)}{\partial t^2} - \overline{c}^2 \frac{\partial^2 p'(x,t)}{\partial x^2} = (c_\mathrm{p} - 1)\frac{\partial q'(x,t)}{\partial t}, \tag{A.2}$$

where p is pressure, $\overline{c}$ is the mean speed of sound, c_p denotes the specific heat, and q denotes the heat-release rate per unit volume.

Appendix B

State-Space realisation

The linear Fractional Transform, henceforth abbreviated LFT, offers a framework to rearrange all interconnected systems in a unified way and therefore can be analysed and synthesised with similar techniques. Figure B.1 describes a LFT with a coefficient matrix P and a controller K

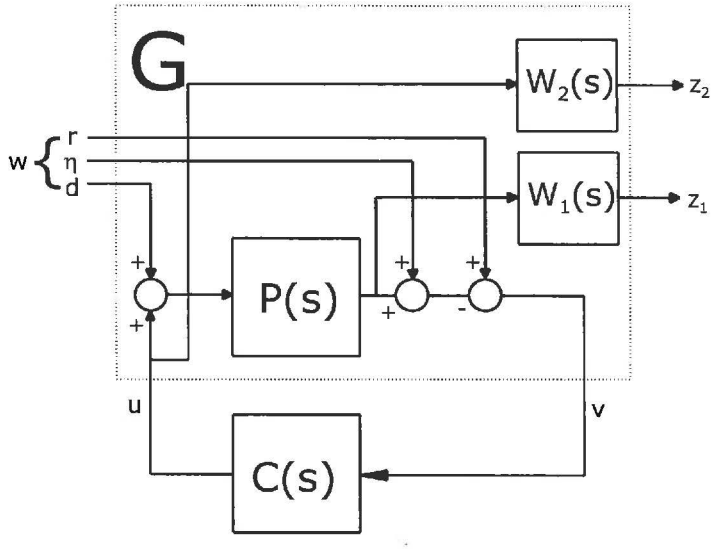

Figure B.1: *feedback control configuration*

The transfer function matrix $G(s)$ has the following structure:

$$G(s) = \begin{pmatrix} 0 & W_1(s)P(s) & 0 & W_1(s)P(s) \\ 0 & 0 & 0 & W_2(s) \\ I & -P(s) & -I & -P(s) \end{pmatrix}$$

The state space realization for each component (except the controller) is given by:

$$P = \begin{pmatrix} A_\mathrm{p} & B_\mathrm{p} \\ C_\mathrm{p} & D_\mathrm{p} \end{pmatrix}, \qquad W_1 = \begin{pmatrix} A_\mathrm{e} & B_\mathrm{e} \\ C_\mathrm{e} & D_\mathrm{e} \end{pmatrix}, \qquad W_2 = \begin{pmatrix} A_\mathrm{u} & B_\mathrm{u} \\ C_\mathrm{u} & D_\mathrm{u} \end{pmatrix}$$

The following relations can be derived, assumed is that d and η are 0:

$$\dot{x}_\mathrm{p} = A_\mathrm{p}x_\mathrm{p} + B_\mathrm{p}u, \qquad y_\mathrm{p} = C_\mathrm{p}x_\mathrm{p} + D_\mathrm{p}u$$

$$\dot{x}_\mathrm{e} = A_\mathrm{e}x_\mathrm{e} + B_\mathrm{e}(r - y_\mathrm{p}), \qquad z_1 = y_\mathrm{e} = C_\mathrm{e}x_\mathrm{e} + D_\mathrm{e}(r - y_\mathrm{p})$$

$$\dot{x}_u = A_u x_u + B_u y_p, \qquad z_2 = y_u = C_u x_u + D_u y_p$$

After elimination of y_p we get:

$$\dot{x}_e = A_e x_e + B_e r - B_e C_p x_p - B_e D_p u, \qquad z_1 = y_e = C_e x_e + D_e r D_e C_p x_p - D_e D_p u$$

$$\dot{x}_u = A_u x_u + B_u C_p x_p - B_u D_p u, \qquad z_2 = y_u = C_u x_u + D_u C_p x_p - D_u D_p u$$

Choose a new state-vector: $\dot{x} = [x_p \; x_e \; x_u]^T$
A representation for $G(A, B, C, D)$ will then be:

$$A = \begin{pmatrix} A_p & 0 & 0 \\ -B_e C_p & A_e & 0 \\ B_u C_p & 0 & A_u \end{pmatrix}$$

$$B_1 = \begin{pmatrix} 0 \\ B_e \\ 0 \end{pmatrix}, \qquad B_2 = \begin{pmatrix} B_p \\ -B_e D_p \\ B_u D_p \end{pmatrix}$$

$$C_1 = \begin{pmatrix} -D_e C_p & C_e & 0 \\ D_u C_p & 0 & C_u \end{pmatrix}, \qquad C_2 = (-C_p \; 0; \; 0)$$

$$D_{11} = \begin{pmatrix} D_e \\ 0 \end{pmatrix}, \qquad D_{12} = \begin{pmatrix} -D_e D_p \\ D_u D_p \end{pmatrix}$$

$$D_{21} = I, \qquad D_{22} = -D_p$$

Finally G(s) will be represented by:

$$G = \begin{pmatrix} A_p & 0 & 0 & 0 & B_p \\ -B_e C_p & A_e & 0 & B_e & -B_e D_p \\ B_u C_p & 0 & A_u & 0 & B_u D_p \\ -D_e C_p & C_e & 0 & D_e & -D_e D_p \\ D_u C_p & 0 & C_u & 0 & D_u D_p \\ -C_p & 0 & 0 & I & -D_p \end{pmatrix}$$

The transfer function matrix G(s) is of the form:

$$G \stackrel{s}{=} \left(\begin{array}{c|cc} A & B_1 & B_2 \\ \hline C_1 & D_{11} & D_{12} \\ C_2 & D_{21} & D_{22} \end{array}\right)$$

The following standard assumptions have to hold to synthesise a controller:

- (A, B_2) is stabilisable and (C_2, A) is detectable;
- $\begin{pmatrix} A - i\omega I & B_2 \\ C_1 & D_{12} \end{pmatrix}$ has full column rank;
- $\begin{pmatrix} A - i\omega I & B_1 \\ C_2 & D_{21} \end{pmatrix}$ has full column rank;
- $D_{12}^T D_{12} = I$ and $D_{12} D_{12}^T = I$.